https://doi.org/10.5194/bg-2019-385
Preprint. Discussion started: 14 October 2019
© Author(s) 2019. CC BY 4.0 License.

Biogeosciences Discussions

The carbon footprint of a Malaysian tropical reservoir: measured versus modeled estimates highlight the underestimated key role of downstream processes

Cynthia Soued[1], Yves T. Prairie[1]

[1]Groupe de Recherche Interuniversitaire en Limnologie et en Environnement Aquatique (GRIL), Département des Sciences Biologiques, Université du Québec à Montréal, Montréal, H2X 3X8, Canada.

Correspondence to: Cynthia Soued (cynthia.soued@gmail.com)

Abstract. Reservoirs are important sources of greenhouse gases (GHG) to the atmosphere and their number is rapidly increasing, especially in tropical regions. Accurately predicting their current and future emissions is essential but hindered by fragmented data on the subject, which often fail to include all emission pathways (diffusion, ebullition, degassing, and downstream emissions) and the high spatial and temporal flux variability. Here we conducted a comprehensive sampling of Batang Ai reservoir (Malaysia), and compared field-based versus modeled estimates of its annual carbon footprint for each emission pathway. Carbon dioxide (CO_2) and methane (CH_4) diffusive fluxes were higher in upstream reaches. Reducing spatial and temporal sampling resolution resulted in up to 64 and 28 % change in flux estimate respectively. Most GHGs present in discharged water were degassed at the turbines, and the remainder were gradually emitted along the outflow river, leaving time for CH_4 to be partly oxidized to CO_2. Overall, the reservoir emitted 2 639 $gCO_2eq\ m^{-2}\ yr^{-1}$, with 90 % occurring downstream of the dam, mostly in the form of CH_4. These emissions, largely underestimated by predictions, are mitigated by CH_4 oxidation upstream and downstream of the dam, but could have been drastically reduced by slightly raising the water intake elevation depth. CO_2 diffusion and CH_4 ebullition were lower than predicted, whereas modeled CH_4 diffusion was accurate. Investigating latter discrepancies, we conclude that exploring morphometry, soil type, and stratification patterns as predictors can improve modeling of reservoir GHG emissions at local and global scales.

1 Introduction

Reservoirs provide a variety of services to humans (water supply, navigation, flood control, hydropower) and cover an estimated area exceeding 0.3 million km^2 globally (Lehner et al., 2011). This area is increasing, with an expected rapid growth of the hydroelectric sector in the next two decades (International Hydropower Association (IHA), 2015), mainly in tropical and subtropical regions (Zarfl et al., 2015). The flooding of terrestrial landscapes can change its carbon (C) balance into significant greenhouse gas (GHG) sources to the atmosphere (Prairie et al., 2018; Rudd et al., 1993; Teodoru et al., 2012). While part of reservoir GHG emissions would occur naturally (not legitimately attributable to damming), the remainder results from newly created environments favoring C mineralization, particularly methane (CH_4) production (flooded organic-rich anoxic soils) (Prairie et al., 2018). Field studies have revealed a wide range in measured fluxes, with spatial and temporal variability sometime spanning several orders of magnitude within a single reservoir (Paranaíba et al.,

https://doi.org/10.5194/bg-2019-385
Preprint. Discussion started: 14 October 2019
© Author(s) 2019. CC BY 4.0 License.

2018; Sherman and Ford, 2011). Moreover, reservoirs can emit GHG through several pathways: surface diffusion at the air-water interface, ebullition from the sediments, and for some reservoirs (mostly hydroelectric) through degassing upon water discharge and downstream emissions of excess gas in the outflow river. The relative contribution of these flux pathways to total emissions is extremely variable. While diffusion is the most frequently sampled, it is often not the main emission pathway (Demarty and Bastien, 2011). Indeed, measured ebullition, degassing, and downstream emissions range from negligible to several order of magnitude higher than diffusion in different reservoirs (Bastien and Demarty, 2013; DelSontro et al., 2010; Galy-Lacaux et al., 1997; Keller and Stallard, 1994; Kemenes et al., 2007; Teodoru et al., 2012; Venkiteswaran et al., 2013), making it a challenge to model total reservoirs GHG emissions.

Literature syntheses over the past 20 years have yielded highly variable global estimates of reservoirs GHG footprint, ranging from 0.5 to 2.3 $PgCO_2eq.yr^{-1}$ (Barros et al., 2011; Bastviken et al., 2011; Deemer et al., 2016; St. Louis et al., 2000). These estimates are based on global extrapolations of averages of sampled systems, representing an uneven spatial distribution biased toward North America and Europe, and an uneven mixture of emission pathways. Recent studies have highlighted the lack of spatial and temporal resolution as well as the frequent absence of some flux pathways (especially degassing, downstream, and N_2O emissions) in most reservoir GHG assessments (Beaulieu et al., 2016; Deemer et al., 2016). More recently, studies have focused on identifying drivers of reservoir GHG flux variability. Using global empirical data, Barros et al. (2011) proposed the first quantitative models for reservoir carbon dioxide (CO_2) and CH_4 surface diffusion as a negative function of reservoir age, latitude, and mean depth (for CO_2 only), and a positive function of dissolved organic carbon (DOC) inputs (Barros et al., 2011). An online tool (G-res) for predicting reservoir C emissions was later developed on the basis of a similar empirical modeling approach of measured reservoir fluxes with globally available environmental data (UNESCO/IHA, 2017). Modeling frameworks to predict GHG emissions from existing and future reservoirs are essential tools for reservoir management. However, their accuracy is directly related to available information and inherently affected by gaps and biases of the published literature. For example, while the G-res model predicts reservoir CO_2 and CH_4 diffusion as well as CH_4 ebullition and degassing on the basis of temperature, age, % littoral zone and soil organic C, it does not consider N_2O emissions, CO_2 degassing, and emissions in the downstream river due to scarcity of data. Overall, the paucity of comprehensive empirical studies limits our knowledge of reservoir GHG dynamics at a local scale, introducing uncertainties in large scale estimates and hindering model development.

The research reported here focusses on building a comprehensive assessment of GHG fluxes of Batang Ai, a tropical reservoir in south-east Asia (Malaysia), over four sampling campaigns spanning two years with an extensive spatial coverage. The main objective of this study is to provide a comprehensive account of CO_2, CH_4 and N_2O fluxes from diffusion, ebullition, degassing, and downstream river (accounting for riverine CH_4 oxidation) to better understand what shapes their relative contributions and their potential mitigation. The second objective is to compare our measured values with modeled estimates from each pathway and gas species to locate where the largest discrepancies are, and thereby identify research avenues for improving the current modeling framework.

https://doi.org/10.5194/bg-2019-385
Preprint. Discussion started: 14 October 2019
© Author(s) 2019. CC BY 4.0 License.

2 Materials and methods

2.1 Study site and sampling campaigns

Batang Ai is a hydroelectric reservoir located on the Borneo Island in the Sarawak province of Malaysia (latitude 1.16º and longitude 111.9º). The regional climate is tropical equatorial with a relatively constant temperature throughout the year, on average 23ºC in the morning to 32ºC during the day. Annual rainfall varies between 3300 and 4600 mm with two monsoon seasons: November to February (northeast monsoon), and June to October (southwest) (Sarawak Government, 2019). Batang Ai reservoir was impounded in 1985 with no prior clearing of the vegetation, and has a dam wall of 85 m in height, a mean depth of 34 m, and a total area of 68.4 km^2. The reservoir catchment consists of 1149 km^2 of mostly forested land where human activities are limited to a few traditional habitations and associated croplands, and localized aquaculture sites within the reservoir main basin. The reservoir has two major inflows: the Batang Ai and Engkari rivers, which flow into two reservoir branches merging upstream of the main reservoir basin (Figure 1). Four sampling campaigns were conducted: 1) November 14th to December 5th 2016 (Nov-Dec 2016), 2) April 19th to May 3th 2017 (Apr-May 2017), 3) February 28th to March 13th 2018 (Feb-Mar 2018), and 4) August 12th to 29th 2018 (Aug 2018).

2.2 Water chemistry

Surface concentrations of DOC, total phosphorus (TP), total nitrogen (TN), and chlorophyll a (Chla) were measured at all surface diffusion sampling sites (Figure 1) and during each campaign. For TP and TN, we collected non-filtered water in acid-washed glass vials stored at 4°C until analysis. TP was measured by spectrophotometry using the standard molybdenum blue method after persulphate digestion. TN analyses were performed by alkaline persulphate digestion to NO_3, subsequently measured on an Alpkem Flow Solution IV autoanalyser. Water filtered at 0.45 µm was used for DOC analysis with a Total Organic Carbon analyser 1010-OI following sodium persulphate digestion. Chla was analysed through spectrophotometry following filtration on Whatman (GF/F) filters and extraction by hot 90 % ethanol solution.

2.3 Surface diffusive flux

Surface diffusion of CO_2 and CH_4 to the atmosphere were measured at 36 sites in the reservoir and 3 sites in the inflow rivers (Figure 1), and sampling of the same sites was repeated each campaign (with a few exceptions). Fluxes were measured using a static air tight floating chamber connected in a closed loop to an Ultraportable gas Analyser (UGGA from LGR). Diffusive flux rates (F_{gas}) were derived from the linear change in CO_2 and CH_4 partial pressures (continuously monitored at 1 Hz for a minimum of 5 min) through time inside the chamber using the following Eq. (1):

$$F_{gas} = \frac{s\,V}{mV\,S}, \quad (1)$$

https://doi.org/10.5194/bg-2019-385
Preprint. Discussion started: 14 October 2019
© Author(s) 2019. CC BY 4.0 License.

Where *s* is the gas accumulation rate in the chamber, V = 25 L the chamber volume, S = 0.184 m^2 the chamber surface area, and *mV* the gas molar volume at current atmospheric pressure.

N_2O diffusive flux was estimated at 7 of the sampled sites (Figure 1) using the following Eq. (2) (Lide, 2005):

$$F_{gas} = k_{gas}\left(C_{gas} - C_{eq}\right), \quad (2)$$

where k_{gas} is the gas exchange coefficient (m d^{-1}), C_{gas} is the gas concentration in the water and C_{eq} is the theoretical gas concentration at equilibrium given measured water temperature, atmospheric pressure and ambient gas concentration. C_{N2O} was measured using the headspace technique, with a 1.12 L sealed glass serum bottle containing surface water and a 0.12 L headspace of ambient air. After shaking the bottle for two minutes to achieve air-water equilibrium, the headspace gas was extracted from the bottle with an airtight syringe and injected in previously evacuated 9 mL glass vial capped with an air tight butyl stopper and aluminium seal. Three analytical replicates and a local sample of ambient air were taken at each site and analysed by gas chromatography using a Shimadzu GC-2040, with a Poropaq Q column to separate gases and an ECD detector. k_{N2O} was derived from the measured k_{CH4} using the following Eq. (3) (Cole and Caraco, 1998; Ledwell, 1984):

$$k_{N2O} = \left(\frac{Sc_{N2O}}{Sc_{CH4}}\right)^{-0.67} k_{CH4}, \quad (3)$$

where Sc is the gas Schmidt number (Wanninkhof, 1992), k_{CH4} was calculated by rearranging Eq. (2) for CH_4, with known values of F_{gas}, C_{gas}, and C_{eq}. CH_4 and CO_2 concentrations in the water were measured using the headspace technique. Surface water was collected in a 60 mL gas-tight plastic syringe in which a 30 mL headspace was created (using either ambient air or carbon free air). The syringe was shaken for 2 min to achieve air-water gas equilibrium. The gas phase was then injected in a 12 mL air-tight pre-evacuated vial and subsequently analysed on a Shimadzu GC-8A Gas chromatograph with flame ionization detector. The samples were also analyzed for isotopic $\delta^{13}CO_2$ and $\delta^{13}CH_4$ signatures using a Cavity Ring Down Spectrometer (CRDS) equipped with a Small Sample Isotopic Module (SSIM, Picarro G2201 -i, Picarro Inc).

2.4 Ebullition flux

Sediment gas ebullition was measured at four sites in the reservoir and two sites in the inflows (Figure1) by deploying 0.785 m^2 underwater inverted funnel traps at 2 to 3 m deep for approximately 20 days in the reservoir and 1h in the inflows. The top part of a closed plastic syringe was fixed to the narrow end of the funnel trap where the emerging bubbles accumulated. Upon recovery, bubble gas volume was measured, collected from the syringe, and injected in 12 mL pre-evacuated air tight vials for CO_2 and CH_4 concentration analyses (using the aforementioned method). Ebullition rate was calculated assuming the original bubble composition was similar to bubbles collected almost right after ascent in the inflows sites, which was 100 % CH_4. Hence we considered CO_2 and N_2O ebullition to be null.

In order to estimate the potential for sediment accumulation fueling ebullition in the littoral zone, we calculated the mud energy boundary depth (EBD, below which fine grained sediments accumulation occurs) using the reservoir surface area (E in km^2) as the exposure parameter in the following Eq. (4) (Rowan et al., 1992):

https://doi.org/10.5194/bg-2019-385
Preprint. Discussion started: 14 October 2019
© Author(s) 2019. CC BY 4.0 License.

$$EBD = 2.685\ E^{0.305}, \tag{4}$$

2.5 Downstream emissions and CH_4 oxidation

Downstream emissions of CO_2 and CH_4 were calculated using the following Eq. (5):

$$F_d = Q\ (C_{up} - C_{base}), \tag{5}$$

Where F_d is the flux to the atmosphere, Q is the water discharge, C_{up} is the gas concentration upstream of the dam at the water withdrawal depth, and C_{base} is the gas concentration considered as a natural baseline in the outflow river (previous to reservoir construction). Since no measurements of pre-impoundment gas concentration are available, we considered two values as upper and lower bonds for C_{base}: 1) the gas concentration at the surface of the reservoir right upstream of the dam, and 2) the gas concentration in the outflow 19 km downstream of the dam. Degassing emissions (gas emitted right after water discharge due to pressure release) were calculated with Eq. (5) replacing C_{base} by the gas concentration measured at the powerhouse right after water discharge. To define C_{up}, we measured in each campaign, CO_2 and CH_4 concentrations in a vertical profile right upstream of the dam at each one to three meters from 0 up to 32 m using a multi-parameter probe equipped with depth, oxygen, and temperature sensors (Yellow Spring Instruments, YSI model 600XLM-M) attached to a 12 Volt submersible Tornado pump (Proactive Environmental Products) for water collection. Gas concentration and $\delta^{13}C$ were measured as previously described. The water withdrawal depth ranged from 20 to 23 m and was estimated based on known values of water intake and water level elevations compared to sea level. C_{up} was defined as the average measured gas concentrations in the range of ± 1 m of the withdrawal depth. Gas concentration was measured at four locations in the outflow, at 0 (power house), 0.6, 2.7, and 19 km downstream of the dam.

Estimates of downstream CH_4 oxidation were obtained, for each sampling campaign, by calculating the fraction of CH_4 oxidized (F_{ox}) using the following Eq. (6):

$$F_{ox} = \frac{-\left(ln(\delta^{13}CH_{4resid}+1000) - \ln\left(\delta^{13}CH_{4source}+1000\right)\right)\left(1-\frac{[CH_4]_{resid}}{[CH_4]_{source}}\right)}{\left(1-\frac{1}{\alpha}\right)\ln\left(\frac{[CH_4]_{resid}}{[CH_4]_{source}}\right)}\ , \tag{6}$$

Eq. (6) is based on a non-steady state isotopic model developed considering evasion (emission to the atmosphere) and oxidation as the two loss processes for CH_4 in the outflow river, assuming negligible isotopic fractionation for evasion (Knox et al., 1992) and a fractionation of α = 1.02 for oxidation (Coleman et al., 1981) (see derivation in Supplementary Information). $[CH_4]_{source}$, $[CH_4]_{resid}$, $\delta^{13}CH_{4source}$, and $\delta^{13}CH_{4resid}$ are the concentrations of CH_4 and their corresponding isotopic signatures at the beginning of the outflow (km 0) and 19 km downstream, representing the source and residual pools of CH_4 respectively. The amount of CH_4 oxidized to CO_2 along the 19 km of river stretch for each sampling campaign was calculated as the product of F_{ox} and $[CH_4]_{source}$. Note that downstream N_2O emissions were considered null since N_2O concentrations measured in the deep reservoir layer were lower than concentrations in the outflow.

https://doi.org/10.5194/bg-2019-385
Preprint. Discussion started: 14 October 2019
© Author(s) 2019. CC BY 4.0 License.

2.6 Ecosystem scale C footprint

Batang Ai annual C footprint was calculated as the sum of surface diffusion, ebullition, and downstream emissions of CO_2, CH_4, and N_2O considering a greenhouse warming potential of 1, 34, and 298 respectively over a 100 years lifetime period (Myhre et al., 2013). For each flux pathway, annual flux was estimated as the average of the sampling campaigns. Ecosystem scale estimate of surface diffusion was calculated for each campaign as the average of measured flux rates applied to the reservoir area for N_2O, and for CO_2 and CH_4 it was obtained by spatial interpolation of measured fluxes over the reservoir area based on inverse distance weighting with a power of two (a power of one yields similar averages, CV < 11 %) using package gstat version 1.1-6 in the R version 3.4.1 software (Pebesma, 2004; R Core Team, 2017). Ebullition at the reservoir scale was calculated as the average of measured reservoir ebullition rates applied to the littoral area (< 3 m deep). The estimated C emissions of Batang Ai based on measured data was compared to values derived from the G-res model (UNESCO/IHA, 2017) and the model presented in Barros et al. (2011). Details on models equations and input variables are presented in the Supplementary Information (Table S2 and S3).

3 Results and discussion

3.1 Water chemistry

The reservoir is stratified throughout the year with a thermocline around 13 m and mostly anoxic conditions in the hypolimnion of the main basin (Figure S1). The system is oligotrophic, with very low concentrations of DOC, TP, TN, and Chla averaging 0.9 mg L^{-1}, 5.9, 0.11, and 1.3 µg L^{-1} respectively (Table S1), and high water transparency (Secchi depth > 5 m). In the reservoir inflows, concentrations of measured chemical species are slightly higher but still in the oligotrophic range (Table S1), however the transparency is much lower due to turbidity (Secchi < 0.5).

3.2 Surface diffusion

Measured CO_2 diffusion in the reservoir averaged 7.7 mmol m^{-2} d^{-1} (Table S1), which is on the low end compared to other reservoirs (Deemer et al., 2016) and even to natural lakes (Sobek et al., 2005), but similar to CO_2 fluxes measured in two reservoirs in Laos (Chanudet et al., 2011). CO_2 diffusion across all sites ranged from substantial uptake to high emissions (from -30.8 to 593.9 mmol m^{-2} d^{-1}, Table S1) reflecting a large spatial and temporal variability. Spatially, CO_2 fluxes measured in the main basin and branches had similar averages of 7.9 and 7.3 mmol m^{-2} d^{-1} respectively, contrasting with higher and more variable values in the inflows (mean of 137.3 mmol.m^{-2}.d^{-1}, Figures 2). Within the reservoir, CO_2 fluxes were variable (SD ± 18.2 mmol m^{-2} d^{-1}) but did not follow a consistent pattern, and might reflect pre-flooding landscape heterogeneity (Teodoru et al., 2011). Temporally, highest average reservoir CO_2 fluxes were measured in Apr-May 2017, when no CO_2 uptake was observed, contrary to other campaigns, especially Feb-Mar and Aug 2018, when CO_2 uptake was

https://doi.org/10.5194/bg-2019-385
Preprint. Discussion started: 14 October 2019
© Author(s) 2019. CC BY 4.0 License.

common (Figure S2) and average Chla concentrations were the highest. This reflects the important role of metabolism (namely CO_2 consumption by primary production) in modulating surface CO_2 fluxes in Batang Ai.

All measured CH_4 diffusive fluxes were positive and ranged from 0.03 to 113.4 mmol m^{-2} d^{-1} (Table S1). Spatially, CH_4 fluxes were progressively higher moving further upstream (Figure 2 and S3) with decreasing water depth and increasing connection to the littoral. This gradient in morphometry induces an increasingly greater contact of the water with bottom and littoral sediments, where CH_4 is produced, explaining the spatial pattern of CH_4 fluxes. CH_4 diffusive fluxes also varied temporally, but to a lesser extent than CO_2, being on average highest in Aug 2018 in the reservoir and in Nov-Dec 2016 in the inflows.

Reservoir N_2O diffusive fluxes (measured with a limited spatial resolution) averaged -0.2 (SD ± 2.1) nmol m^{-2} d^{-1} (Table S1). The negative value indicates that the system acts as a slight net sink of N_2O, absorbing an estimated 2.1 gCO_2eq m^{-2} yr^{-1} (Table 2). Atmospheric N_2O uptake have previously been reported in aquatic systems and linked to low oxygen and nitrogen content conducive to complete denitrification which consumes N_2O (Soued et al., 2016; Webb et al., 2019). These environmental conditions match observations in Batang Ai, with a low average TN concentration of 0.11 mg L^{-1} (Table S1) and anoxic deep waters (Figure S1).

3.3 Ebullition

We calculated that CH_4 ebullition rates in Batang Ai's littoral area ranged from 0.02 to 0.84 mmol m^{-2} d^{-1}, which contrasts with rates measured in its inflows that are several orders of magnitude higher (52 and 103 mmol m^{-2} d^{-1}). Similar patterns were observed in other reservoirs, where inflow arms where bubbling hot spots due to a higher organic C supply driven by terrestrial matter deposition (DelSontro et al., 2011; Grinham et al., 2018). Since ebullition rates are notoriously heterogeneous and were measured at only four sites in the reservoir, they may not reflect ecosystem-scale rates. However, our attempt to manually provoke ebullition at several other sites (by physically disturbing the sediments) did not result in any bubble release, confirming the low potential for ebullition in the reservoir littoral zone. Moreover, we calculated that fine grained sediment accumulation is unlikely at depths shallower than 9.7 m (estimated EBD) in Batang Ai. This, combined with the reservoir steep slope, prevents the sustained accumulation of organic material in littoral zones (Blais and Kalff, 1995), hence decreasing the potential for CH_4 production and bubbling there. Also, apparent littoral sediment composition in the reservoir; dense clay with low porosity, may further hinder bubble formation and emission (de Mello et al., 2018).

3.4 Degassing and downstream emissions

Emissions downstream of the dam, expressed on a reservoir-wide areal basis, ranged from 19.3 to 38.6 mmol m^{-2} d^{-1} for CO_2 and from 5.9 to 13.9 mmol m^{-2} d^{-1} for CH_4 (Table 1). The amount of CO_2 exiting the reservoir varied little between sampling campaigns (CV = 3 %) contrary to CH_4 (CV = 28 %, Table 1 and Figure 3). Higher temporal variability of CH_4 concentration in discharged water is likely modulated by microbial CH_4 oxidation in the reservoir water column upstream of the dam. Evidence of high CH_4 oxidation are apparent in reservoir water column profiles, showing a sharp decline of CH_4

https://doi.org/10.5194/bg-2019-385
Preprint. Discussion started: 14 October 2019
© Author(s) 2019. CC BY 4.0 License.

concentration and increase of $\delta^{13}CH_4$ right around the water withdrawal depth (Figure S1). This vertical pattern results from higher oxygen availability when moving up in the hypolimnion (Figure S1), promoting CH_4 oxidation at shallower depths. Once GHGs have exited the reservoir, a large fraction (40 and 65 % for CO_2 and CH_4 respectively) is immediately lost to the atmosphere as degassing emissions (Table 1), which is in line with previous literature reports (Kemenes et al., 2016). Along the outflow river, CO_2 and CH_4 concentrations gradually decreased, $\delta^{13}CO_2$ remained stable, whereas $\delta^{13}CH_4$ steadily increased indicating riverine CH_4 oxidation (Figure 3). We estimated that riverine CH_4 oxidation ranged from 0.38 to 1.80 mmol m^{-2} d^{-1} (expressed per m^2 of reservoir area for comparison), transforming 18 to 32 % (depending on the sampling campaign) of the CH_4 to CO_2 within the first 19 km of the outflow. Riverine oxidation rates did not co-vary temporally with water temperature, oxygen availability, or CH_4 concentrations (known as typical drivers (Thottathil et al., 2019)), hence they might be regulated by other factors like light and microbial assemblages (Murase and Sugimoto, 2005; Oswald et al., 2015). Overall, riverine oxidation of CH_4 to CO_2 (which has a 34 times lower warming potential) reduced radiative forcing of downstream emissions (excluding degassing) by, on average, 18 %, and the total annual reservoir C footprint by 6 %. Despite having a measurable impact on reservoir C emissions, CH_4 oxidation downstream of dams was only estimated in two other reservoirs to our knowledge (Guérin and Abril, 2007; Kemenes et al., 2007). Accounting for this process is particularly important in systems where downstream emissions are large, a common situation in tropical reservoirs (Demarty and Bastien, 2011). While additional data on the subject is needed, our results provide one of the first basis for understanding CH_4 oxidation downstream of dams, and eventually integrating this component to global models (from which it is currently absent).

3.5 Importance of sampling resolution

High spatial and temporal sampling resolution have been recently highlighted as an important but often lacking aspect of reservoir C footprint assessments (Deemer et al., 2016; Paranaíba et al., 2018). Reservoir scale fluxes are usually derived from applying an average of limited flux measurements to the entire reservoir area. For Batang Ai, this method overestimates by 14 % (130 gCO_2eq m^{-2} yr^{-1}) and 64 % (251 gCO_2eq m^{-2} yr^{-1}) CO_2 and CH_4 diffusive fluxes respectively compared to spatial interpolation. This is due to the effect of extreme values that are very constrained in space but have a disproportionate effect on the overall flux average. Also, reducing temporal sampling resolution to one campaign instead of four changes the reservoir C footprint estimate by up to 28 %. An additional source of uncertainty in reservoir flux estimates is the definition of a baseline value representing natural river emissions in order to calculate downstream emissions of excess gas in the outflow attributable to damming. In Batang Ai, downstream emission was estimated on the basis of a potential range in natural baseline emissions, however, measured values of GHG concentrations in the pre-impounded river would have substantially reduced the estimate uncertainty. Results from Batang Ai reinforce the importance of pre and post-impoundment sampling resolution and upscaling methods in annual reservoir-scale GHG flux estimates.

https://doi.org/10.5194/bg-2019-385
Preprint. Discussion started: 14 October 2019
© Author(s) 2019. CC BY 4.0 License.

3.6 Reservoir C footprint and potential mitigation

Most of Batang Ai emissions occur downstream of the dam through degassing (60.2 %) and from the outflow river surface (29.7 %), while surface diffusive fluxes contributed only 10.0 %, and ebullition 0.13 % (Table 2). In all pathways, CH_4 fluxes were higher than CO_2 and N_2O (especially for degassing), accounting for 76.7 % of Batang Ai CO_2eq emissions. This distribution of the flux can be attributed mostly to the accumulation of large quantities of CH_4 in the hypolimnion, combined with the fact that the withdrawal depth is located within this layer, allowing the accumulated gas to escape to the atmosphere. Previous studies on reservoirs with similar characteristics to Batang Ai (tropical climate with a permanent thermal stratification and deep water withdrawal) have also found degassing and downstream emissions to be the major emission pathways, especially for CH_4 (Galy-Lacaux et al., 1997; Kemenes et al., 2007).

Overall, we estimated that the reservoir emits on average 2 639 (± 651) $gCO_2eq\ m^{-2}\ yr^{-1}$ which corresponds to 0.181 $TgCO_2eq\ yr^{-1}$ over the whole system. In comparison, the annual areal emission rate (diffusion and ebullition) of the inflows, based on a more limited sampling resolution, is estimated to range from 10.8 to 52.5 $kgCO_2eq\ m^{-2}\ yr^{-1}$, mainly due to extremely high ebullition. When applied to the approximated surface area of the river before impoundment (1.52 km^2), this rate translates to 0.016 – 0.080 $TgCO_2eq$ (Table 2), assuming a similar flux rates in the current inflows and pre-impoundment river. While the emission rate of the river per unit of area is an order of magnitude higher than for the reservoir, its estimated total flux remains 2.3 to 11.3 times lower due to a much smaller surface. Higher riverine emissions rates are probably due to a shallower depth and higher inputs of terrestrial organic matter, both conducive to CO_2 and CH_4 production and ebullition. Changing the landscape hydrology to a reservoir drastically reduced areal flux rates, especially ebullition, however, it widely expanded the volume of anoxic environments (sediments and hypolimnion), creating a vast new space for CH_4 production. The new hydrological regime also created an opportunity for the large quantities of gas produced in deep layers to easily escape to the atmosphere through the outflow and downstream river.

One way to reduce reservoir emissions is to ensure low GHG concentrations at the turbine water withdrawal depth. In Batang Ai, maximum CO_2 and CH_4 concentrations are found in the reservoir deep layers, and rapidly decrease from 20 to 10 m for CO_2 and from 25 to 15 m for CH_4 (Figure S1). This pattern is commonly found in lakes and reservoirs and results from thermal stratification and biological processes (aerobic respiration and CH_4 oxidation). Knowing this concentration profile, degassing and downstream emissions could have been reduced in Batang Ai by elevating the water withdrawal depth to avoid hypolimnetic gas release. We calculated that elevating the water withdrawal depth by 1, 3, and 5 m would result in a reduction of degassing and downstream emissions by 1, 13, and 22 % for CO_2 and by 27, 89, and 98 % for CH_4, respectively (Figure S4). Consequently, a minor change in the dam design could have drastically reduced Batang Ai's C footprint. This should be taken in consideration in future reservoir construction, especially in tropical regions.

https://doi.org/10.5194/bg-2019-385
Preprint. Discussion started: 14 October 2019
© Author(s) 2019. CC BY 4.0 License.

3.7 Measured versus modeled fluxes

Based on measurements, Batang Ai emits on average 113 (± 15) $gCO_2eq\ m^{-2}\ yr^{-1}$ via surface CO_2 diffusion. This value is 41 times lower than predicted by Barros et al. model (4671 $gCO_2eq\ m^{-2}\ yr^{-1}$, Table 2) based on reservoir age, DOC inputs (derived from DOC water concentration), and latitude. The high predicted value for Batang Ai, being a relatively old reservoir with very low DOC concentration, is mainly driven by its low latitude. While reservoirs in low latitudes globally have higher average CO_2 fluxes due to higher temperature and often dense flooded biomass (Barros et al., 2011; St. Louis et al., 2000), our results provide a clear example that not all tropical reservoirs have high CO_2 emissions by simple virtue of their geographical location. Despite high temperature, Batang Ai's very low water organic matter content (Table S1) offers little substrate for net heterotrophy, and its strong permanent stratification creates a physical barrier potentially retaining CO_2 derived from flooded biomass in the hypolimnion.

In comparison, the G-res model predicts a diffusive CO_2 flux of 577 (509-655) $gCO_2eq\ m^{-2}\ yr^{-1}$, which includes the flux naturally sustained by catchment carbon inputs (397 $gCO_2eq\ m^{-2}\ yr^{-1}$, predicted flux 100 years after flooding) and the flux derived from organic matter flooding (180 $gCO_2eq\ m^{-2}\ yr^{-1}$). While the predicted G-res value is much closer than that predicted from the Barros et al. model, it still overestimates measured flux, mostly the natural baseline (catchment derived) part of it. The G-res predicts baseline CO_2 effluxes as a function of soil C content, a proxy for C input to the reservoir. While Batang Ai soil is rich in organic C (~50 g kg^{-1}), it also has a high clay content (> 40 %) (ISRIC - World Soil Information, 2019; Wasli et al., 2011) which is known to bind with organic matter and reduce its leaching to the aquatic environment (Oades, 1988). This may explain the unusually low DOC concentration in the reservoir and its inflows (0.3 to 1.8 mg L^{-1}, Table S1) that are among the lowest reported in freshwaters globally (Sobek et al., 2007). Had G-res been able to capture the baseline emissions more correctly in Batang Ai (close to zero given the very low DOC inputs), predictions would have nearly matched observations. Finally, the G-res model is not suitable to predict CO_2 uptake, which was observed in 32 % of flux measurements in Batang Ai due to an occasionally net autotrophic surface metabolism favored under low C inputs (Bogard and del Giorgio, 2016). The modeling framework of reservoirs diffusive CO_2 flux would benefit from a better predictive capacity of internal metabolism and catchment C inputs in a diverse range of landscape properties.

Our field-based estimate of Batang Ai CH_4 surface diffusion is 153 (± 43) $gCO_2eq\ m^{-2}\ yr^{-1}$, which differs by only 5 % and 15 % from the G-res and Barros et al. modeled predictions of 161 (132-197) and 176 $gCO_2eq\ m^{-2}\ yr^{-1}$ respectively (Table 2). Both models use as predictors age, a proxy for water temperature (air temperature or latitude), and an indicator of reservoir morphometry (% littoral area or mean depth), and Barros et al. also uses DOC input (Table S3). Similar predictors were identified in a recent global literature analysis, which also pointed out the role of trophic state in CH_4 diffusion, with Batang Ai falling well in the range of flux reported in other oligotrophic reservoirs (Deemer et al., 2016). Overall, our results show that global modelling frameworks for CH_4 diffusive emissions capture reasonably well the reality of Batang Ai.

Measured estimate of reservoir-scale CH_4 ebullition averaged 3.4 (± 1.9) $gCO_2eq\ m^{-2}\ yr^{-1}$ (Table 2), which is one of the lowest reported globally in reservoirs (Deemer et al., 2016), and is an order of magnitude lower than the 52 (32 - 83) gCO_2eq

https://doi.org/10.5194/bg-2019-385
Preprint. Discussion started: 14 October 2019
© Author(s) 2019. CC BY 4.0 License.

m^{-2} yr^{-1} predicted by the G-res model (the only available model for reservoir ebullition). This contrasts with the perception that tropical reservoirs consistently have high ebullitive emissions, and support the idea that the supply of sediment organic matter, rather than temperature, is the primary driver of ebullition (Grinham et al., 2018). Batang Ai sediment properties and focusing patterns mentioned earlier could explain the model overestimation of CH_4 ebullition. The G-res model considers the fraction of littoral area and horizontal radiance (a proxy for heat input) as predictors of ebullition rate, but does not integrate other catchment properties. Building a stronger mechanistic understanding of the effect of sediment composition and accumulation patterns on CH_4 bubbling may improve our ability to more accurately predict reservoir ebullition flux.

Our empirical estimate shows that 503 (± 66) and 1869 (± 518) gCO_2eq m^{-2} yr^{-1} are emitted as CO_2 and CH_4 respectively downstream of the dam (including degassing), accounting for 90 % of Batang Ai C emission (Table 2). Currently there are no available model predicting downstream C emissions from reservoirs, except the G-res model which is able to predict only the CH_4 degassing part of this flux. Modeled CH_4 degassing in Batang Ai is 468 (266-832) gCO_2eq m^{-2} yr^{-1} compared to an estimated 1342 (± 372) gCO_2eq m^{-2} yr^{-1} based on our measurements. Predictive variables used to model CH_4 degassing are modeled CH_4 diffusive fluxes (based on % littoral area and temperature) and water retention time (Table S3). In Batang Ai, the strong and permanent stratification favors oxygen depletion in the hypolimnion which promotes deep CH_4 accumulation combined with a decoupling between surface and deep water layers. The model relies strongly on surface CH_4 patterns to predict excess CH_4 in the deep layer, which could explain why it underestimates CH_4 degassing in Batang Ai. Improving this aspect of the model requires a better capacity to predict CH_4 accumulation in deep reservoir layers based on globally available data. In this regard, our results suggest that the role of stratification is a promising key element to investigate.

3.8 Conclusions

The comprehensive GHG portrait of Batang Ai highlights the importance of spatial and temporal sampling resolution and the inclusion of all flux components in reservoir GHG assessments. Gas dynamics downstream of the dam (degassing, outflow emissions and CH_4 oxidation), commonly not assessed in reservoir GHG studies, are major elements in Batang Ai. We suggest that these emissions could have been greatly diminished with a minor change to the dam design (withdrawal depth decrease). Mitigating GHG emissions from future reservoirs depends on the capacity to predict GHG fluxes from all pathways. In this regard, the comparison between Batang Ai measured and modeled GHG flux estimates allowed us to identify knowledge gaps based on which we propose the four following research avenues. 1) Refine the modeling of reservoir CO_2 diffusion by studying its link with metabolism and organic matter leaching from different soil types. 2) Examine the potential for CH_4 ebullition in littoral zones in relation to patterns of organic matter sedimentation linked to morphometry. 3) Improve the modeling of CH_4 degassing by better defining drivers of hypolimnetic CH_4 accumulation, namely thermal stratification. 4) Gather additional field data on GHG dynamics downstream of dams (degassing, river emissions, and river CH_4 oxidation) in order to incorporate all components of the flux to the modeling of reservoirs C footprint.

https://doi.org/10.5194/bg-2019-385
Preprint. Discussion started: 14 October 2019
© Author(s) 2019. CC BY 4.0 License.

Author contribution

CS contributed to conceptualization, methodology, validation, formal analysis, investigation, data curation, writing - original draft, writing – review and editing, and project administration. YTP contributed to Methodology, validation, investigation, resources, writing – review and editing, supervision, and funding acquisition.

Acknowledgment

This work was funded by Sarawak Energy Berhad and the Natural Science and Engineering Research Council of Canada (Discovery grant to Y.T.P. and BES-D scholarship to C.S.). This is a contribution to the UNESCO chair in Global Environmental Change and the GRIL. We are grateful to Karen Lee Suan Ping and Jenny Choo Cheng Yi for their logistic support and participation in sampling campaigns. We also thank Jessica Fong Fung Yee, Amar Ma'aruf Bin Ismawi, Gerald Tawie Anak Thomas, Hilton Bin John, Paula Reis, Sara Mercier-Blais and Karelle Desrosiers for their help on the field, and Katherine Velghe and Marilyne Robidoux for their assistance during laboratory analyses.

Competing interests

The authors declare that they have no conflict of interest.

https://doi.org/10.5194/bg-2019-385
Preprint. Discussion started: 14 October 2019
© Author(s) 2019. CC BY 4.0 License.

References

Barros, N., Cole, J. J., Tranvik, L. J., Prairie, Y. T., Bastviken, D., Huszar, V. L. M., del Giorgio, P. and Roland, F.: Carbon emission from hydroelectric reservoirs linked to reservoir age and latitude, Nat. Geosci., 4(9), 593–596, doi:10.1038/ngeo1211, 2011.

Bastien, J. and Demarty, M.: Spatio-temporal variation of gross CO2 and CH4 diffusive emissions from Australian reservoirs and natural aquatic ecosystems, and estimation of net reservoir emissions, Lakes Reserv. Res. Manag., 18(2), 115–127, doi:10.1111/lre.12028, 2013.

Bastviken, D., Tranvik, L. J., Downing, J. A., Crill, P. M. and Enrich-Prast, A.: Freshwater Methane Emissions Offset the Continental Carbon Sink, Science (80-.)., 331(6013), 50–50, doi:10.1126/science.1196808, 2011.

Beaulieu, J. J., McManus, M. G. and Nietch, C. T.: Estimates of reservoir methane emissions based on a spatially balanced probabilistic-survey, Limnol. Oceanogr., 61(S1), S27–S40, doi:10.1002/lno.10284, 2016.

Blais, J. M. and Kalff, J.: The influence of lake morphometry on sediment focusing, Limnol. Oceanogr., 40(3), 582–588, doi:10.4319/lo.1995.40.3.0582, 1995.

Bogard, M. J. and del Giorgio, P. A.: The role of metabolism in modulating CO2 fluxes in boreal lakes, Global Biogeochem. Cycles, 30(10), 1509–1525, doi:10.1002/2016GB005463, 2016.

Chanudet, V., Descloux, S., Harby, A., Sundt, H., Hansen, B. H., Brakstad, O., Serça, D. and Guerin, F.: Gross CO2 and CH4 emissions from the Nam Ngum and Nam Leuk sub-tropical reservoirs in Lao PDR, Sci. Total Environ., 409(24), 5382–5391, doi:10.1016/j.scitotenv.2011.09.018, 2011.

Cole, J. J. and Caraco, N. F.: Atmospheric exchange of carbon dioxide in a low-wind oligotrophic lake measured by the addition of SF6, Limnol. Oceanogr., 43(4), 647–656, doi:10.4319/lo.1998.43.4.0647, 1998.

Coleman, D. D., Risatti, J. B. and Schoell, M.: Fractionation of carbon and hydrogen isotopes by methane-oxidizing bacteria, Geochim. Cosmochim. Acta, 45(7), 1033–1037, doi:10.1016/0016-7037(81)90129-0, 1981.

Deemer, B. R., Harrison, J. A., Li, S., Beaulieu, J. J., DelSontro, T., Barros, N., Bezerra-Neto, J. F., Powers, S. M., dos Santos, M. A. and Vonk, J. A.: Greenhouse Gas Emissions from Reservoir Water Surfaces: A New Global Synthesis, Bioscience, 66(11), 949–964, doi:10.1093/biosci/biw117, 2016.

DelSontro, T., McGinnis, D. F., Sobek, S., Ostrovsky, I. and Wehrli, B.: Extreme Methane Emissions from a Swiss Hydropower Reservoir: Contribution from Bubbling Sediments, Environ. Sci. Technol., 44(7), 2419–2425,

doi:10.1021/es9031369, 2010.

DelSontro, T., Kunz, M. J., Kempter, T., Wüest, A., Wehrli, B. and Senn, D. B.: Spatial Heterogeneity of Methane Ebullition in a Large Tropical Reservoir, Environ. Sci. Technol., 45(23), 9866–9873, doi:10.1021/es2005545, 2011.

Demarty, M. and Bastien, J.: GHG emissions from hydroelectric reservoirs in tropical and equatorial regions: Review of 20 years of CH4 emission measurements, Energy Policy, 39(7), 4197–4206, doi:10.1016/j.enpol.2011.04.033, 2011.

Galy-Lacaux, C., Delmas, R., Jambert, C., Dumestre, J.-F., Labroue, L., Richard, S. and Gosse, P.: Gaseous emissions and oxygen consumption in hydroelectric dams: A case study in French Guyana, Global Biogeochem. Cycles, 11(4), 471–483, doi:10.1029/97GB01625, 1997.

Grinham, A., Dunbabin, M. and Albert, S.: Importance of sediment organic matter to methane ebullition in a sub-tropical freshwater reservoir, Sci. Total Environ., 621, 1199–1207, doi:10.1016/j.scitotenv.2017.10.108, 2018.

Guérin, F. and Abril, G.: Significance of pelagic aerobic methane oxidation in the methane and carbon budget of a tropical reservoir, J. Geophys. Res. Biogeosciences, 112(G3), doi:10.1029/2006JG000393, 2007.

International Hydropower Association (IHA): A brief history of hydropower, [online] Available from: https://www.hydropower.org/a-brief-history-of-hydropower (Accessed 11 July 2019), 2015.

ISRIC - World Soil Information: SoilGrids v0.5.3., [online] Available from: https://soilgrids.org/#!/?layer=ORCDRC_M_sl4_250m&vector=1 (Accessed 1 May 2019), 2019.

Keller, M. and Stallard, R. F.: Methane emission by bubbling from Gatun Lake, Panama, J. Geophys. Res., 99(D4), 8307, doi:10.1029/92JD02170, 1994.

Kemenes, A., Forsberg, B. R. and Melack, J. M.: Methane release below a tropical hydroelectric dam, Geophys. Res. Lett., 34(12), 1–5, doi:10.1029/2007GL029479, 2007.

Kemenes, A., Forsberg, B. R. and Melack, J. M.: Downstream emissions of CH4 and CO2 from hydroelectric reservoirs (Tucuruí, Samuel, and Curuá-Una) in the Amazon basin, Inl. Waters, 6(3), 295–302, doi:10.1080/IW-6.3.980, 2016.

Knox, M., Quay, P. D. and Wilbur, D.: Kinetic isotopic fractionation during air-water gas transfer of O2 , N2 , CH4 , and H2, J. Geophys. Res., 97(C12), 20335, doi:10.1029/92JC00949, 1992.

Ledwell, J. J.: The Variation of the Gas Transfer Coefficient with Molecular Diffusity, in Gas Transfer at Water Surfaces,

https://doi.org/10.5194/bg-2019-385
Preprint. Discussion started: 14 October 2019
© Author(s) 2019. CC BY 4.0 License.

pp. 293–302, Springer Netherlands, Dordrecht., 1984.

Lehner, B., Liermann, C. R., Revenga, C., Vörösmarty, C., Fekete, B., Crouzet, P., Döll, P., Endejan, M., Frenken, K., Magome, J., Nilsson, C., Robertson, J. C., Rödel, R., Sindorf, N. and Wisser, D.: High- resolution mapping of the world's reservoirs and dams for sustainable river- flow management, Front. Ecol. Environ., 9(9), 494–502, doi:10.1890/100125, 2011.

Lide, D.: CRC Handbook of Chemistry and Physics, edited by CRC Press, Boca Raton, FL. [online] Available from: http://www.hbcpnetbase.com, 2005.

St. Louis, V. L., Kelly, C. a., Duchemin, É., Rudd, J. W. M. and Rosenberg, D. M.: Reservoir Surfaces as Sources of Greenhouse Gases to the Atmosphere: A Global Estimate, Bioscience, 50(9), 766, doi:10.1641/0006-3568, 2000.

de Mello, N. A. S. T., Brighenti, L. S., Barbosa, F. A. R., Staehr, P. A. and Bezerra Neto, J. F.: Spatial variability of methane (CH4) ebullition in a tropical hypereutrophic reservoir: silted areas as a bubble hot spot, Lake Reserv. Manag., 34(2), 105–114, doi:10.1080/10402381.2017.1390018, 2018.

Murase, J. and Sugimoto, A.: Inhibitory effect of light on methane oxidation in the pelagic water column of a mesotrophic lake (Lake Biwa, Japan), Limnol. Oceanogr., 50(4), 1339–1343, doi:10.4319/lo.2005.50.4.1339, 2005.

Myhre, G., Shindell, D., Bréon, F.-M., Collins, W., Fuglestvedt, J., Huang, J., Koch, D., Lamarque, J.-F., Lee, D., Mendoza, B., Nakajima, T., Robock, A., Stephens, G., Takemura, T. and Zhang, H.: Anthropogenic and Natural Radiative Forcing, in Climate Change 2013: The Physical Science Basis. Contribution of Working Group I to the Fifth Assessment Report of the Intergovernmental Panel on Climate Change, pp. 659–740, Cambridge, United Kindom. [online] Available from: http://www.climatechange2013.org/images/report/WG1AR5_Chapter08_FINAL.pdf, 2013.

Oades, J. M.: The retention of organic matter in soils, Biogeochemistry, 5(1), 35–70, doi:10.1007/BF02180317, 1988.

Oswald, K., Milucka, J., Brand, A., Littmann, S., Wehrli, B., Kuypers, M. M. M. and Schubert, C. J.: Light-Dependent Aerobic Methane Oxidation Reduces Methane Emissions from Seasonally Stratified Lakes, edited by C. Lovejoy, PLoS One, 10(7), e0132574, doi:10.1371/journal.pone.0132574, 2015.

Paranaíba, J. R., Barros, N., Mendonça, R., Linkhorst, A., Isidorova, A., Roland, F., Almeida, R. M. and Sobek, S.: Spatially Resolved Measurements of CO2 and CH4 Concentration and Gas-Exchange Velocity Highly Influence Carbon-Emission Estimates of Reservoirs, Environ. Sci. Technol., 52(2), 607–615, doi:10.1021/acs.est.7b05138, 2018.

Pebesma, E. J.: Multivariable geostatistics in S: the gstat package, Comput. Geosci., 30(7), 683–691, doi:10.1016/j.cageo.2004.03.012, 2004.

Prairie, Y. T., Alm, J., Beaulieu, J., Barros, N., Battin, T., Cole, J., del Giorgio, P., DelSontro, T., Guérin, F., Harby, A., Harrison, J., Mercier-Blais, S., Serça, D., Sobek, S. and Vachon, D.: Greenhouse Gas Emissions from Freshwater Reservoirs: What Does the Atmosphere See?, Ecosystems, 21(5), 1058–1071, doi:10.1007/s10021-017-0198-9, 2018.

R Core Team: R: A language and environment for statistical computing, [online] Available from: https://www.r-project.org/, 2017.

Rowan, D. J., Kalff, J. and Rasmussen, J. B.: Estimating the Mud Deposition Boundary Depth in Lakes from Wave Theory, Can. J. Fish. Aquat. Sci., 49(12), 2490–2497, doi:10.1139/f92-275, 1992.

Rudd, J., Harris, R. and Kelly, C. A.: Are Hydroelectric Reservoirs Signficant Sources of Greenhouse Gases?, Ambio, 22(4), 246–248 [online] Available from: http://www.jstor.org/stable/4314078?seq=1#page_scan_tab_contents, 1993.

Sarawak Government: The Geography of Sarawak, [online] Available from: https://www.sarawak.gov.my/web/home/article_view/159/176/ (Accessed 3 May 2019), 2019.

Sherman, B. and Ford, P.: Methane Emissions from Two reservoirs in a steep, sub- Tropical rainforest catchment, in Science Forum and Stakeholder Engagement: Building Linkages, Collaboration and Science Quality, edited by D. K. Begbie and S. L. Wakem, pp. 1–9, Urban Water Security Research Alliance, Brisbane, Queensland., 2011.

Sobek, S., Tranvik, L. J. and Cole, J. J.: Temperature independence of carbon dioxide supersaturation in global lakes, Global Biogeochem. Cycles, 19(2), n/a–n/a, doi:10.1029/2004GB002264, 2005.

Sobek, S., Tranvik, L. J., Prairie, Y. T., Kortelainen, P. and Cole, J. J.: Patterns and regulation of dissolved organic carbon: An analysis of 7,500 widely distributed lakes, Limnol. Oceanogr., 52(3), 1208–1219, doi:10.4319/lo.2007.52.3.1208, 2007.

Soued, C., del Giorgio, P. A. and Maranger, R.: Nitrous oxide sinks and emissions in boreal aquatic networks in Québec, Nat. Geosci., 9(2), 116–120, doi:10.1038/ngeo2611, 2016.

Teodoru, C. R., Prairie, Y. T. and del Giorgio, P. A.: Spatial Heterogeneity of Surface CO2 Fluxes in a Newly Created Eastmain-1 Reservoir in Northern Quebec, Canada, Ecosystems, 14(1), 28–46, doi:10.1007/s10021-010-9393-7, 2011.

Teodoru, C. R., Bastien, J., Bonneville, M.-C., del Giorgio, P. A., Demarty, M., Garneau, M., Hélie, J.-F., Pelletier, L., Prairie, Y. T., Roulet, N. T., Strachan, I. B. and Tremblay, A.: The net carbon footprint of a newly created boreal hydroelectric reservoir, Global Biogeochem. Cycles, 26(2), doi:10.1029/2011GB004187, 2012.

Thottathil, S. D., Reis, P. C. J. and Prairie, Y. T.: Methane oxidation kinetics in northern freshwater lakes, Biogeochemistry, 143(1), 105–116, doi:10.1007/s10533-019-00552-x, 2019.

https://doi.org/10.5194/bg-2019-385
Preprint. Discussion started: 14 October 2019
© Author(s) 2019. CC BY 4.0 License.

UNESCO/IHA: The GHG Reservoir Tool (G- res), [online] Available from: https://g-res.hydropower.org/ (Accessed 1 May 2019), 2017.

Venkiteswaran, J. J., Schiff, S. L., St. Louis, V. L., Matthews, C. J. D., Boudreau, N. M., Joyce, E. M., Beaty, K. G. and Bodaly, R. A.: Processes affecting greenhouse gas production in experimental boreal reservoirs, Global Biogeochem. Cycles, 27(2), 567–577, doi:10.1002/gbc.20046, 2013.

Wanninkhof, R.: Relationship between wind speed and gas exchange over the ocean, J. Geophys. Res., 97(C5), 7373, doi:10.1029/92JC00188, 1992.

Wasli, M. E., Tanaka, S., Kendawang, J. J., Abdu, A., Lat, J., Morooka, Y., Long, S. M. and Sakurai, K.: Soils and Vegetation Condition of Natural Forests and Secondary Fallow Forests within Batang Ai National Park Boundary , Sarawak , Malaysia, Kuroshio Sci., 5(1), 67–76, 2011.

Webb, J. R., Hayes, N. M., Simpson, G. L., Leavitt, P. R., Baulch, H. M. and Finlay, K.: Widespread nitrous oxide undersaturation in farm waterbodies creates an unexpected greenhouse gas sink, Proc. Natl. Acad. Sci., 201820389, doi:10.1073/pnas.1820389116, 2019.

Zarfl, C., Lumsdon, A. E., Berlekamp, J., Tydecks, L. and Tockner, K.: A global boom in hydropower dam construction, Aquat. Sci., 77(1), 161–170, doi:10.1007/s00027-014-0377-0, 2015.

https://doi.org/10.5194/bg-2019-385
Preprint. Discussion started: 14 October 2019
© Author(s) 2019. CC BY 4.0 License.

Table 1: CO_2 and CH_4 dynamics downstream of the dam: gas export rate from upstream to downstream of the dam, degassing, oxidation (production for CO_2 and consumption for CH_4), and resulting total emissions to the atmosphere (expressed as a range of values based on the two different baseline concentrations). Units are in mmol m^{-2} d^{-1} of reservoir surface area.

	GHG downstream of the dam (mmol m^{-2} d^{-1})			
	Exported	Degassed	CO_2 prod. / CH_4 cons. by oxidation	Total emitted
CO_2				
Nov-Dec 2016	40.62	15.26	0.90	27.9 - 38.6
Apr-May 2017	37.80	14.91	0.59	24.7 - 36.1
Feb-March 2018	37.98	9.58	1.80	19.3 - 36.9
Aug 2018	38.07	21.67	0.38	30 - 36.9
CH_4				
Nov-Dec 2016	14.84	11.56	0.90	13.76 - 13.93
Apr-May 2017	7.32	4.00	0.59	5.9 - 6.73
Feb-March 2018	12.47	4.92	1.80	8.91 - 10.67
Aug 2018	10.71	9.54	0.38	10.05 - 10.32

https://doi.org/10.5194/bg-2019-385
Preprint. Discussion started: 14 October 2019
© Author(s) 2019. CC BY 4.0 License.

Table 2: Estimated reservoir and inflow areal and total GHG fluxes to the atmosphere (± standard error or 95 % confidence interval based on model standard error) from different pathways based on measured and modeled approaches.

	Diffusion			**Ebullition**	**Degassing**		**Downstream river emissions**		**Total**
	CO_2	CH_4	N_2O	CH_4	CO_2	CH_4	CO_2	CH_4	
				Flux rate ($gCO_2eq\ m^{-2}\ yr^{-1}$)					
Reservoir (measured)	113 (± 15)	153 (± 43)	-2.1 (± 7.1)	3.4 (± 1.9)	247 (± 32)	1342 (± 372)	256 (± 34)	527 (± 146)	2639 (± 651)
Reservoir (G-res model)	577 (509 - 655)	161 (132 - 197)		52 (32 - 83)		468 (266 - 832)			1258 (1041 - 1636)
Reservoir (Barros et al. model)	4671	176							4847
Inflows (measured)	156 - 9538	248 - 22510	NA	10377 - 20498	0	0	0	0	10781 - 52546
				Total flux ($TgCO_2eq\ yr^{-1}$)					
Reservoir (measured)	0.008	0.010	-0.0001	0.0002	0.017	0.092	0.018	0.036	0.181
River*	0 - 0.014	0 - 0.034	NA	0.016 - 0.031	0.000	0.000	0.000	0.000	0.016 - 0.08

https://doi.org/10.5194/bg-2019-385
Preprint. Discussion started: 14 October 2019
© Author(s) 2019. CC BY 4.0 License.

Biogeosciences Discussions
Open Access
EGU

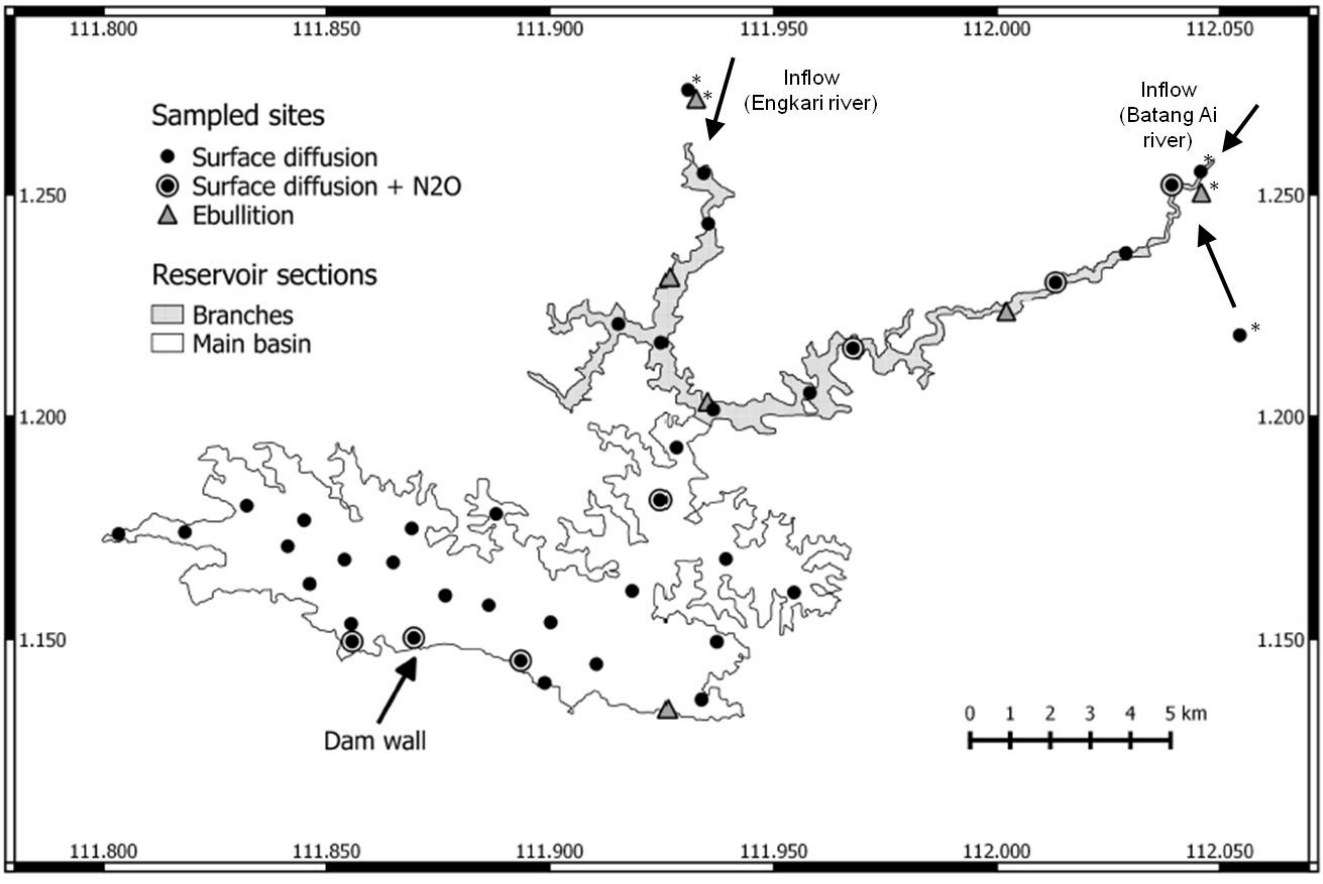

490 **Figure 1: Map of Batang Ai showing the location of sampled sites and reservoir sections. * Represents the reservoir inflow sites.**

https://doi.org/10.5194/bg-2019-385
Preprint. Discussion started: 14 October 2019
© Author(s) 2019. CC BY 4.0 License.

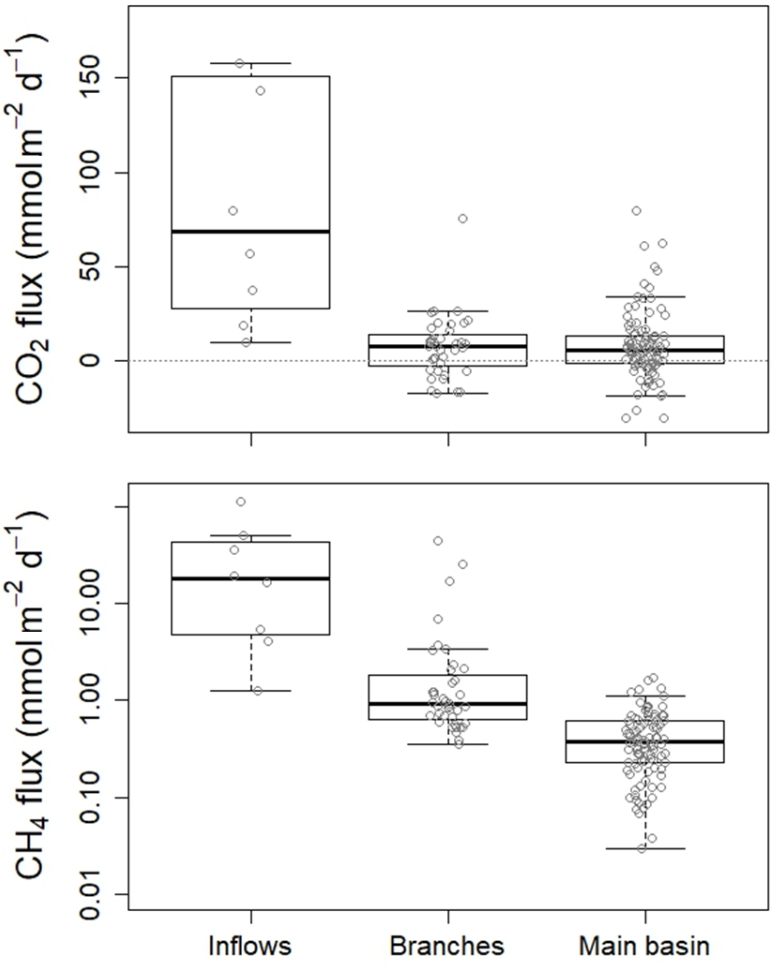

Figure 2: Boxplots of measured CH_4 (on a log axis) and CO_2 fluxes grouped according to spatial position. Boxes are bounded by the 25th and 75th percentile and show medians (solid lines), and whiskers show 10th and 90th percentiles. Gray circles show single data points.

https://doi.org/10.5194/bg-2019-385
Preprint. Discussion started: 14 October 2019
© Author(s) 2019. CC BY 4.0 License.

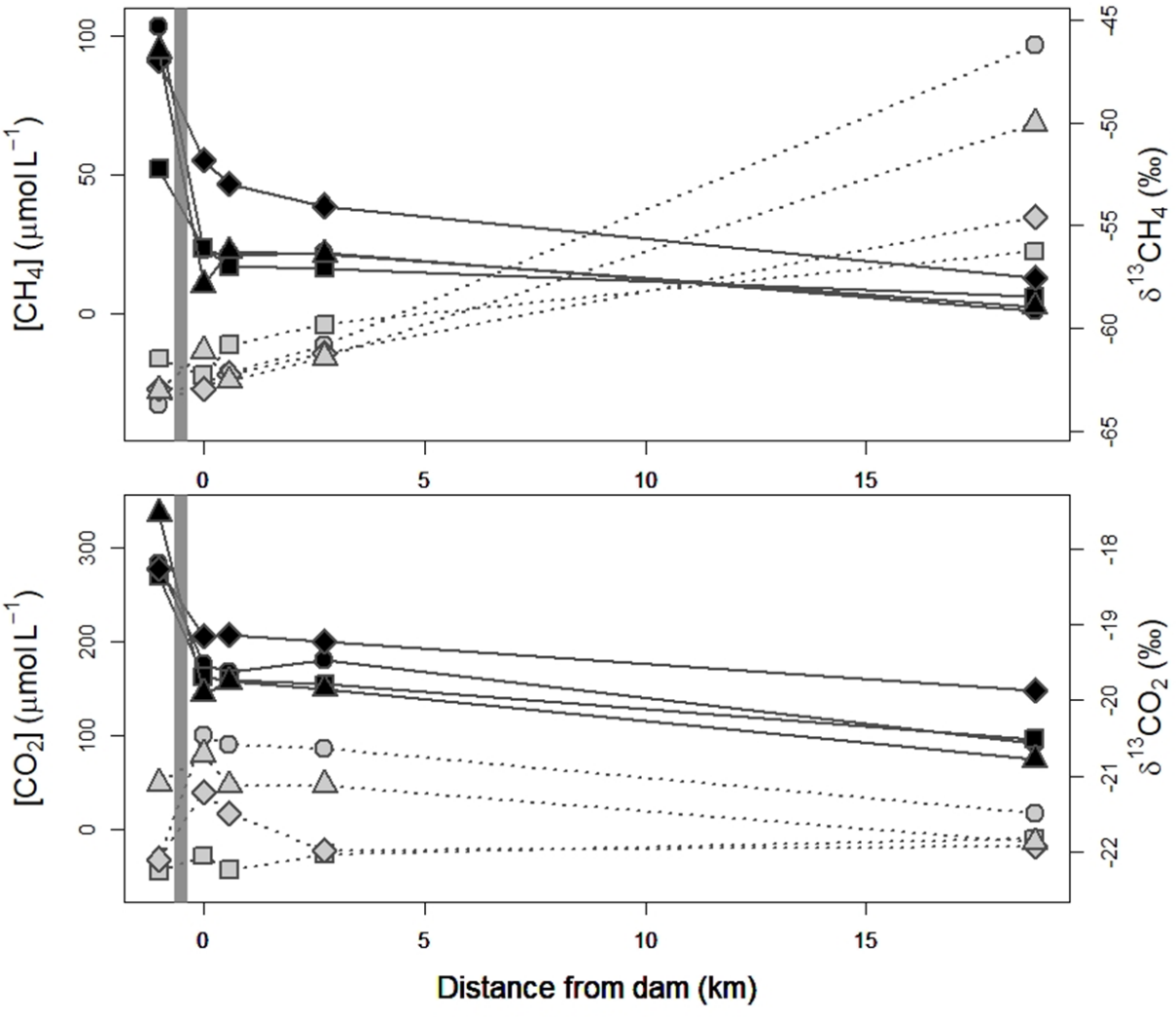

Figure 3: Concentrations (black symbols and solid line) and $\delta^{13}C$ (gray symbols and dotted lines) of CO_2 and CH_4 from right upstream of the dam (gray band) to 19 km downstream in the outflow river. Circles, squares, diamonds, and triangles represent values from Nov-Dec 2016, Apr-May 2017, Feb-Mar 2018, and Aug 2018 respectively.